International Journal for Housing Science and Its Applications
Publish August 10, 2025. Volume 46, Issue 4 Pages 3945-3958

https://doi.org/10.70517/ijhsa464514a

Deep Learning Based Safety Protection Technology and Fault Identification Method for Building DC Distribution System

Gaohua Man[1,*], Ting Li[1] and Gengqiang Huang[1]
[1] School of Green Building and Low Carbon Technology, Guangxi Technological College of Machinery and Electricity, Nanning, Guangxi, 530007, China
Corresponding authors: (e-mail: mangaohua202301@163.com).

Abstract In order to meet the demand for electricity in buildings, this project combines the DC power distribution equipment for buildings currently available on the market, and utilizes AC/DC converters (AC/DC), DC buses, distributed power supplies, DC loads, accumulators, switches, and protection devices to jointly complete the design scheme of the DC power distribution system for buildings. The corresponding fault feature quantities are extracted using the generalized S-transform as the input samples of the gated cyclic unit network, and the Adam optimization algorithm is used to optimize the model operation for the problem of accuracy degradation that may easily occur during the training process, while the safety protection technology based on the gated cyclic unit network is formulated. A science and technology park is selected as the case of this construction project, and the model is used to analyze the case. When Eline is greater than Ebus and EP is greater than EN, the model correctly recognizes a negative bus fault, corresponding to the R-value of [0,1,0,0,0,1,0], and the model repairs this type of fault by means of circuit breaker tripping. Even under the influence of transition resistance, the safety protection scheme of building DC distribution system in this paper still performs excellent.

Index Terms building construction, building DC distribution system, fault identification, safety protection scheme, gated cyclic unit network

I. Introduction

Accompanied by the development of semiconductor technology and power electronics technology, DC distribution system has gradually become a research hotspot in various countries for its technical advantages such as being able to efficiently and reliably access DC loads, distributed energy generation and energy storage units [1]-[3]. DC distribution system can interconnect a large number of distributed power sources and energy storage systems through DC grid, directly supplying power to DC loads, or through power electronic converters, accessing AC loads, distributed power sources and AC power grids, and as the importance of the DC distribution system continues to highlight, its safety protection technology and fault identification methods have also attracted much attention [4]-[7].

DC distribution protection technology is one of the key technologies in the development of DC distribution. Unlike the traditional AC power distribution system which has mature and proven protection technology, the research of DC distribution protection technology is still in its infancy, and there is no actual experience and standard of DC distribution system protection configuration [8]-[11]. The protection technology, as the application bottleneck of DC distribution, is still in the theoretical research stage. Generally speaking, the protection of DC distribution network can be divided into three aspects: protection equipment, protection strategy and fault diagnosis, which should be coordinated and interdependent [12]-[15]. And in order to accelerate the fault recovery speed, reduce the customer outage time, and improve the reliability of the distribution network, it is also necessary to accurately locate the fault point and troubleshoot the fault, reduce the pressure of reversing operation and manual patrolling, and meet the requirements of the development of intelligent distribution network [16]-[19]. Although the DC distribution network has a short line distance, the method of manual patrol to find the fault point is almost difficult to realize. Therefore, it is of great significance to conduct research on rapid fault identification and accurate and reliable fault localization for DC distribution networks [20]-[23].

This paper uses the generalized S-transform method, which has a better extraction effect, to realize the accurate capture of fault characteristics, ensure the scientific and comprehensive conclusions of the study, and also improve the slow convergence speed of the gated cyclic unit network and local fitting problems. Based on the perspective of building electricity demand, the corresponding hardware is utilized to construct the building DC power distribution system, and the DC bus voltage control principle is also outlined. Based on the generalized S-transform method, the data of this study is collected, and the data is set as the input of the gated cyclic unit network, and in order to

improve the convergence speed of the model algorithm in the early stage, the learning rate decay strategy and the Adam optimization algorithm are introduced. Based on the protection initiation criterion, the protection program design task based on the gated recurrent unit network is completed, taking a science and technology park as an example, and using the gated recurrent unit network to explore the effectiveness of the system's safety protection and fault identification in an all-round way.

II. DC distribution system safety protection and fault identification

II. A.Exploration of Building DC Distribution Systems

DC power distribution system is divided into unipolar and bipolar structure. Compared with AC power distribution, DC power distribution has the characteristics of simple form, easy control, high transmission efficiency, renewable energy and other distributed power sources can be flexibly and efficiently connected to the system, and unified deployment and control to improve the large-scale application and consumption of renewable energy. The voltage of the DC distribution system can be regulated at ±30%, and the power voltage can be adjusted according to the characteristics of the electrical equipment, if the power side adopts the electrical equipment with intelligent adjustment, the equipment can adjust its power according to the change of DC bus voltage, and the flexibility of the energy demand of the real terminal has gradually changed from the past "source with load" to "load with source" to adjust the energy consumption of the building.

II. A. 1) Building distribution load composition

Building electricity can be divided into the nature of use: residential electricity (residential electricity), residential public auxiliary power electricity (such as residential public lighting, elevators, sewage pumps, etc.), community auxiliary power (such as car pools, pump rooms, heat exchange stations, fire pump rooms, information rooms, etc., ancillary buildings, community street lights, monitoring, access control systems, etc.). Different nature of electricity consumption by different power distribution room is responsible for power supply, the residents by the low-base power distribution room power supply, community supporting by the high-base power distribution room power supply.

II. A. 2) Selection of DC distribution voltage

Building low-voltage distribution system for a single large capacity load or important loads such as: elevator machine room, fixed communications equipment room and other equipment using radial power supply, for general loads using trunk and radial combination of power supply. Household power distribution is supplied in the form of trunking, with trunking cables leading from the distribution room and then branching out for distribution on each floor, and the loads carried by the trunking are mostly greater than 14kW. Common areas carry smaller loads, typically between 5kW and 22kW.

Most of the household electrical appliances ultimately in the form of DC power supply, household appliances DC transformer there are two levels of differentiation degree, portable low-power devices, such as cell phones, electric fans, computers, etc., the converted DC voltage between 12V ~ 110V, high-power devices, such as air conditioners, water heaters, washing machines, etc., the converted DC voltage between 295V ~ 450V, daily life of household inverter type appliances, DC voltage The DC voltage of daily household inverter appliances is between 310V and 400V, and the voltage of small power appliances is between 20V and 50V.

Comprehensive the above situation within the family DC power distribution should be used DC48V, DC375V dual-voltage power supply to ensure that the equipment works in an efficient ideal voltage, but due to the family's electricity habits, in addition to air conditioning, water heaters, refrigerators and other fixed electrical equipment, power supply by the wall outlet, the rest of the appliances more by the wiring plug for power extension, multiple appliances centralized plug to use the wall AC socket using the AC250V10A specifications, distribution conductor cross-section of 2.5mm², the maximum plug can take 2.5kW electrical load, but the voltage in the DC48V this program with a load of about 0.8kW, it is difficult to meet the existing family power habits, if the amplification of the wire will lead to the increase in pre-buried pipeline, walls, floors will be thickened, improve construction costs. It is recommended to adopt DC distribution system, i.e. DC distribution is adopted between the transformer and distribution room to the regional distribution cabinet, and DC distribution is adopted from the distribution cabinet to the end of the electricity according to the form of loads, so as to ensure the electricity demand of each load.

II. A. 3) General measures for security of building distribution systems

For example, the impact of ambient temperature, reduce the temperature can increase the output power of the transformer and reduce transformer losses, such as the number of transformers and reasonable choice of technical and economic comparisons, etc. are all considerations affecting the selection of transformer capacity. From energy saving, economic, practical, safe and reliable, generally selected transformer load factor in 0.53-0.92 is appropriate. When the power distribution system for three-phase four-wire distribution, its cross-section should be twice the

cross-section of the phase line. Miniature circuit breakers (including leakage circuit breakers) closely without interval installation should be considered to reduce the capacity and test its interception capacity, usually 7 ~ 10 closely without interval installation of about 45% reduction in capacity, the ambient temperature on the switch of the rated current impact can not be ignored, which can be verified from the product's technical data and related information. Socket rated current for known use of equipment should be greater than 1.49 times the rated current of the equipment, unknown use of equipment should not be less than 12.72A.

Prevention of fire leakage current action protector should be set in its protective range of normal leakage current less than or equal to 200mA parts. High-rise buildings, low-voltage power distribution system is mostly three-level distribution, fire leakage protector should be located in the second level of power distribution box switch. For high-rise residential buildings should be set in each residential power inlet main switch to prevent fire leakage protector.

II. B.Components of a building DC distribution system

Currently commercially available distributed power sources of practical use in buildings include building photovoltaic BIPV and elevator regenerative power generation. In the future, there will be more distributed power sources (e.g., micro-gas turbines, wind power, fuel cells, etc.) used in buildings, and the control strategies for different distributed power sources will be different.

II. B. 1) System components and corresponding technical issues

The building DC distribution system composition is shown by Figure 1. By the AC / DC converter (AC / DC), DC bus, distributed power supply, DC loads, accumulators, switches and protection devices (not shown in the figure) 6 parts. AC / DC converter can be composed of 6 IGBT bi-directional converter circuits, the role of which is to provide controlled rectification to the DC bus when the distributed power supply in the building can not meet the DC load power. The rectifier overcomes the low power factor and harmonic problems of traditional diode bridge rectifier circuits, and can achieve PF=1 and minimize EMC harmonics. The AC/DC converter can invert the DC side power to the grid when the distributed power source generates excess power. When the distributed power supply capacity is small, the power grid may not allow the return of power, at this time, the AC / DC converter can be used in a simple structure, inexpensive bridge rectifier circuit, at this time, the power can only be unidirectional transmission to the DC load. The AC/DC converter output should be lower than the DC bus voltage, and put into operation when the bus voltage falls below a set threshold.

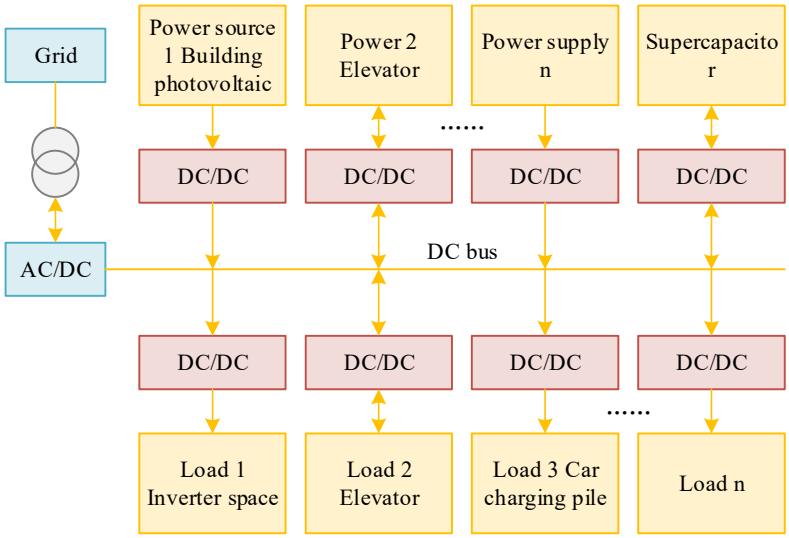

Figure 1: Building DC power distribution system

II. B. 2) DC bus voltage control process

The distributed power supply outputs are protected from static and dynamic circulating currents between the individual power supplies by redundant impedances located inside the DC/DC converter. The accumulator should also be viewed as a distributed power supply, acting as an energy throughput. The output of each power supply uses the same voltage to form a voltage source, and its output power is measured by the output current. When the DC bus voltage fluctuates upward, the DC/DC converter of the accumulator accumulates energy by adjusting the charging current, thus reducing the DC bus voltage and maintaining a constant bus voltage. If the bus voltage

continues to rise when the accumulator is full, the AC/DC feed to the grid should be activated or part of the distributed power supply should be shut down. When the DC bus voltage fluctuates downward, the accumulator discharges to the bus through the DC/DC converter to maintain a constant bus voltage. When the accumulator discharges to the limit value and the bus voltage continues to fall to the minimum threshold of bus voltage, AC/DC puts into rectification work. DC bus voltage fluctuations should be in the millivolt range, otherwise the redundant resistor losses will be too high.

II. C.Fault feature quantity extraction based on generalized S-transform

II. C. 1) Principle of the generalized S-transform

The corresponding fault feature quantities are extracted using the generalized S-transform and used as input samples for the deep learning model. The detailed generalized S-transform principle is explained as follows:

The generalized S transform introduces adjustable factors α and β for higher time-frequency resolution compared to the conventional S transform. The discrete form of the generalized S transform of signal $x(t)$ is shown in equation (1):

$$\begin{cases} S\left[jT,\dfrac{n}{NT}\right]=\sum\limits_{\delta=0}^{N-1}X\left[\dfrac{\delta+n}{NT}\right]e^{\frac{-2\pi^2\delta^2}{\alpha^2n^2}}e^{\frac{i2\pi\delta j}{N}} & n\neq 0 \\ S[jT,0]=\dfrac{1}{N}\sum\limits_{\delta=0}^{N-1}X\left[\dfrac{\delta}{Nt}\right] & n=0 \end{cases} \tag{1}$$

The signal $x(t)$ is generalized S transformed to obtain a complex time-frequency matrix $S[p,q]$ whose row vectors represent the time-domain characteristics of the signal at a particular frequency and the column vectors represent the amplitude-frequency characteristics of the signal at a particular moment in time. Define the transient energy sum E of the generalized S transform of the signal at a particular time-frequency band as:

$$E=\sum_{p=0}^{P}\sum_{q=1}^{Q}\left\{abs\left(S[p,q]\right)\right\}^2 \tag{2}$$

where $abs\left(S[p,q]\right)$ is expressed as the absolute value of the $S[p,q]$ matrix element.

II. C. 2) Fault feature volume extraction

In order to avoid measurement errors and to continuously accumulate the variability of the fault characteristic quantities, the proposed scheme uses the generalized S-transform to extract the transient voltage energy sums in specific frequency bands as the network input quantities.

(1) Fault identification feature quantity

In the initial stage of the fault, using the variability of the high-frequency component of DC voltage and the high-frequency component of bus voltage, the in-zone and out-of-zone fault identification function can be realized.

Select a specific frequency window of 1500~3000Hz and use Eq. (2) to obtain the high-frequency transient energy sum of DC voltage U_{dc12}, E_{line}, and the transient energy sum of bus voltage U_{dc1}, E_{bus}, which are used as the fault identification characteristic quantities. Define the ratio of high-frequency transient energy and $N=E_{line}/E_{bus}$. Line fault, $N>\gamma_H$. Bus fault, $N<\gamma_L$. Out-of-area fault, $\gamma_L<N<\gamma_H$. Where γ_H and γ_L are the high and low thresholds of the fault identification criterion respectively, which are adjusted by the GRU network itself.

(2) Fault selector characteristic quantity

In the initial stage of the fault, the difference between the low-frequency components of the positive and negative reactance voltages can be utilized to realize the fault pole selection function.

Select the data window of a specific frequency band from 0 to 300 Hz and use Eq. (2) to obtain the low-frequency transient energy sum of the positive reactance voltage, E_P, and the low-frequency transient energy sum of the negative reactance voltage, E_N, which are used as the fault selection characteristic quantities. Define the ratio of the low-frequency transient energy sum $M=E_P/E_N$. In case of positive-pole ground fault, $M>\lambda$. In case of negative-pole ground fault, $M<1/\lambda$. In case of bipolar short-circuit fault, $1/\lambda<M<\lambda$. In Eq. λ is the threshold value of the fault selection criterion, which is adjusted by the GRU network itself.

The high-frequency transient energy of the bus voltage and E_{bus}, the high-frequency transient energy of the DC voltage and E_{line}, the low-frequency transient energy of the positive reactance voltage and E_P, and the low-frequency transient energy of the negative reactance voltage and E_N are used as four inputs to the deep learning

model. Using the above fault feature quantities to train the network model, fault identification and fault pole selection functions can be realized.

II. D.Deep learning model based on gated recurrent cell networks

The GRU (gated recurrent unit network) deep learning model has strong nonlinear fitting and feature learning capabilities, which can accurately extract deep fault features from time sample data under the coupling of complex influencing factors, improve the accuracy of fault identification, and enhance the anti-interference capability of the protection scheme.

II. D. 1) Principle of the gated cycle unit

The long short-term memory network's forgetting gates and inputs are merged into a single update, while the data-hidden state and the state of the unit are unified, simplifying the structure of the LSTM, and the simplified structure of the network is called a gated recurrent unit (GRU) The main difference between a gated recurrent unit and a long short-term memory network is that only two control units, the merged update gate and the reset gate, are utilized to control the network's forgetting and updating states [24], [25]. The simplified structure of the gated loop unit not only retains the effect of the long- and short-term memory network, but also makes its internal structure simpler, improves efficiency, and has higher scalability. The loop structure of the gated loop unit is shown in Fig. 2.

Compared with the simplified structure of LSTM the gated loop cell calculation is shown by Eqs. (3) to (6):

$$u_t = \sigma\left(W_{xu}x_t + W_{hu}h_{t-1} + b_u\right) \tag{3}$$

$$r_t = \sigma\left(W_{xr}x_t + W_{tr}h_{t-1} + b_r\right) \tag{4}$$

$$\tilde{h}_t = \phi\left(W_{xh}x_t + W_{rh}\left(r_t \circ h_{t-1}\right) + b_h\right) \tag{5}$$

$$h_t = u_t h_{t-1} + \left(1 - u_t\right) \circ \tilde{h}_t \tag{6}$$

where u_t is the update gate. r_t is the reset gate. x_t is the input vector at time point t. h_{t-1} is the output response at the previous time point. W and b are the weight matrix and bias vector, respectively. σ is the sigmoid function. ϕ is the $\tanh$ function. The update gate controls how much of the current state h_t considers the information referenced from the previous time point state h_{t-1} and how much information is charged from the candidate state h_t, while the reset gate controls whether the candidate state h_t considers the previous time point state in its computation h_{t-1}. The gated loop unit generates a hidden pre-state h_t at each time point, which is also seen as a memory state at each time point, that allows information to flow along the network without losing or bursting elements. At each time point, the current hidden pre-state is iterated through the time points to the next time loop, thus passing the previous useful information backward sequentially, a mechanism that can uncover hidden correlations between information.

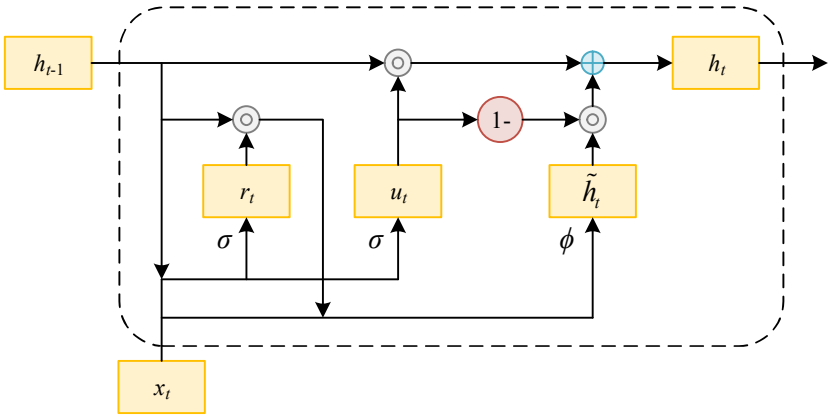

Figure 2: The cycle structure of the gated cycle unit

II. D. 2) Training algorithm for GRU network models

Conventional GRU neural network uses stochastic gradient descent algorithm to iteratively update the weights of the neural network, the convergence speed of this model algorithm in the early stage is slow and it is prone to accuracy degradation [26], [27]. In order to improve the accuracy of prediction and accelerate the convergence speed of the model in the early stage, the paper adopts the Adam optimization algorithm and introduces the learning rate decay strategy to optimize the GRU neural network model.

(1) Adam optimization algorithm

Adam designs independent adaptive learning rates for different parameters by calculating the first-order and second-order moment estimates of the gradient.

The algorithm is as follows:

First, the decay averages for m_t and v_t are computed:

First-order moment estimates:

$$m_t = beta1 \times m_{t-1} + (1 - beta1) \times dx \tag{7}$$

Second-order moment estimation:

$$v_t = beta2 \times v_{t-1} + (1 - beta2) \times (dx)^2 \tag{8}$$

where $beta1$ is the exponential decay rate of the first-order moment estimate. $beta2$ is the exponential decay rate of the second-order moment estimate, and dx is the gradient. The paper makes parameters $beta1 = 0.9$, $beta2 = 0.999$.

The second step performs bias correction, which corrects the first and second moment estimates by calculating the bias.

The bias correction for the first-order moment estimates, second-order moment estimates:

$$m_t' = \frac{m_t}{1 - beta1} \tag{9}$$

$$v_t' = \frac{v_t}{1 - beta2} \tag{10}$$

(2) Learning rate decay strategy in Adam algorithm

The paper introduces the learning rate decay strategy on the basis of Adam algorithm, which can speed up the updating speed of parameters, make Adam algorithm converge faster in the early stage, and can improve the accuracy of the model.

The paper adopts the fractional decay method, and the formula for fractional decay is:

$$alpha_t = \frac{alpha_{t-1}}{1 + decayrate \times epoch} \tag{11}$$

where $epoch$ represents all the data within the sample set trained once. $decayrate$ is the decay rate. The text makes parameters $decayrate = 1$, $epoch = 1$.

As the number of iterations increases, the learning rate will decay in a fractional decay manner, and the global optimal solution is sought through the decayed learning rate. The purpose of using this method is to reduce the oscillation of the convergence curve during the iteration process, improve the convergence speed and stability of the model, and obtain the global optimal solution.

In order to avoid the situation that the learning rate decays to zero when the learning rate decay strategy is used, the minimum learning rate is made to be 0.0001. In the iteration process of the algorithm, when the learning rate is less than 0.0001, the learning rate decay will not be carried out again.

II. D. 3) Improved GRU network model construction

The input of GRU network is a time series, and the training needs to split the normalized data into multiple sub-sequences, which are fed to each input unit separately to extract the temporal feature information, and finally recognized by the classifier. In order to weaken the co-adaptation of neurons and solve the overfitting problem, Dropout layer is introduced in the network. However, Dropout used before the recurrent layer will generate noise and hinder the learning process, so Dropout will be used after the update gate of the GRU, and the same Dropout mask is used for all time steps.

The fully connected layer (Dense) belongs to the feature learning layer, which can change the features extracted from the network in a nonlinear way to improve the learning generalization ability of the network model. Due to the high dimensionality of the power system fault data, which is generally a linear indivisible problem, the SVM classifier is better than the softmax classifier to deal with the effect, therefore, this paper uses the SVM classifier and introduces the Gaussian kernel function. The improved GRU network model is shown in Fig. 3, where $X_i - X_N$ is divided into multiple time sub-sequences, N is the number of sequence steps, and the number of data in each sub-sequence is called the sequence step, $y_i - y_m$ is the output of the GRU network, and $g_i \sim g_n$ is the input of the SVM classifier.

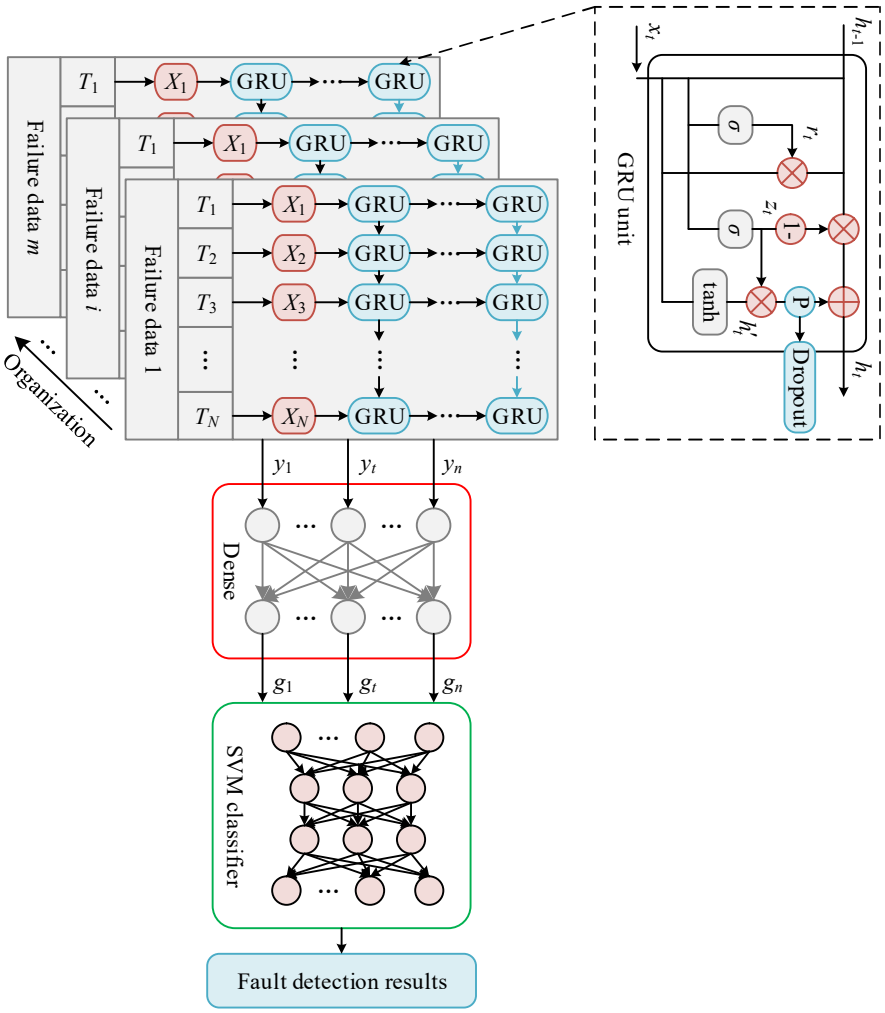

Figure 3: Improved GRU network model

II. E. Protection schemes based on gated cyclic cell networks

II. E. 1) Protection activation criteria

In order to ensure that the protection starts quickly after a fault, and at the same time to avoid repeated detection, this paper utilizes the DC voltage change rate to construct the protection startup criterion:

$$\begin{cases} IdU_{dc} / dt \triangleright \delta_{set} \\ \delta_{set} = k_{set} U_{deN} \end{cases} \tag{12}$$

where δ_{set} is the threshold value of the protection algorithm startup criterion, U_{dcN} is the rated voltage of the DC line, and k_{set} is the constant value coefficient. In order to prevent the false action of the starting element, the protection starting criterion should be established continuously for 0.35ms before confirming the detection of the fault. Since the voltage change rate is susceptible to noise interference and other influences, the startup criterion should be improved subsequently.

II. E. 2) Training and Testing of GRU Network Models

In this paper, E_{bus}, E_{line}, E_P and E_N are used as GRU network input vectors, i.e., $X=\left[E_{bus}E_{line}E_pE_N\right]$, and the deep learning model is trained to realize the fault identification and pole selection functions.

(1) Acquisition of training sample data

In this paper, the selection of sample data takes into account the influence of different fault sections (DC line faults, bus faults and out-of-area faults), different fault locations (0%~100% from the first section), different fault types (positive-pole grounding faults, negative-pole grounding faults and bipolar short-circuit faults), different transition resistances, noise disturbances (50 dB) and distribution capacitances $(0.62\mu F/km)$ in order to ensure that the samples are balanced and sufficient. , and then the adequate sample data are used to train the GRU deep learning model, which extracts and fuses the fault feature information and puts it into the SVM classifier for fault identification and fault pole selection.

(2) Sample data window selection

The higher the sampling frequency, the more obvious the fault sample characteristics, the higher the fit of the network, but the sampling frequency is limited by equipment and other factors. The sampling frequency is selected as 50 kHz. In this paper, we select the voltage data (transient voltage energy sum of specific frequency bands) of 0.68 ms after the fault, i.e., 100 sample point data, at this time, the dimension of input vector X is $n=4\times t\times f=4\times 0.68\times 100=272$.

(3) Sample data preprocessing

Due to the large differences in training data values, the distribution of fault characteristics is not uniform. Therefore, the training dataset X is normalized to maximize the fault features and improve the network training accuracy, Eq:

$$\hat{E}_i=\frac{E_i-\min\left(E_i\right)}{\max\left(E_i\right)-\min\left(E_i\right)} \tag{13}$$

where $\hat{E}_i$ is the normalized sample data (transient energy sum). E_i is the original sample data. $\min$ and $\max$ denote the minimum and maximum values of E_i. The preprocessed sample input vector is:

$$X=\left[\hat{E}_{bus}\hat{E}_{line}\hat{E}_p\hat{E}_N\right] \tag{14}$$

For training, the sample data is divided into multiple time sub-sequences, where the number of sequence steps is 50 and the step length is 4. Take $\hat{E}_{bus}=\left[\hat{E}_{bus1}\hat{E}_{bus2}\ldots\hat{E}_{busb}\right]$ as an example, where b is the number of data $(b=60)$, after dividing it into multiple time sub-sequences, $\hat{E}_{bus}=\left[\hat{E}_{bus1}\hat{E}_{bus2}\ldots\hat{E}_{busN}\right]$, N is the number of sequence steps $(N=15)$, and the step length of each time sub-sequence vector $\hat{E}_{busN}$ is 15, and the multiple time sub-sequences are put into the GRU unit for training.

(4) Fault detection

After offline training of the deep learning model is completed, the model is saved, and after a fault occurs, the startup criterion is established, the protection is started, and the sample data are collected and processed to obtain the sample input vector X, which is then fed into the saved GRU model, and the model outputs the results after calculation. The six outputs of the network model are line fault, bus fault, out-of-area fault, positive fault, negative fault and bipolar fault, i.e., network output $R=\left[R_1R_2R_3R_4R_5R_6\right]$, and the outputs are represented by “1” and “0”. After successful fault detection, the corresponding protection action needs to be initiated, based on the protection scheme of the gated loop unit network as shown in Figure 4.

III. Example analysis of a building DC power distribution system

III. A. Overview of construction works

At present, medium and high voltage DC transformers and other equipment are still immature and expensive in terms of economy and reliability, so medium and high voltage DC distribution grids are not as economical and reliable as traditional AC distribution grids. However, low-voltage DC equipment has been relatively mature, and although the current medium and high voltage DC distribution is still in the demonstration and validation stage, it can be expected that in the future there will be more projects adopting DC distribution, i.e., buildings will be introduced from the municipal grid to the DC power supply. The article takes a science and technology park as an example, and uses a network of gated circulating units to explore the effectiveness of the system in terms of security protection and fault identification.

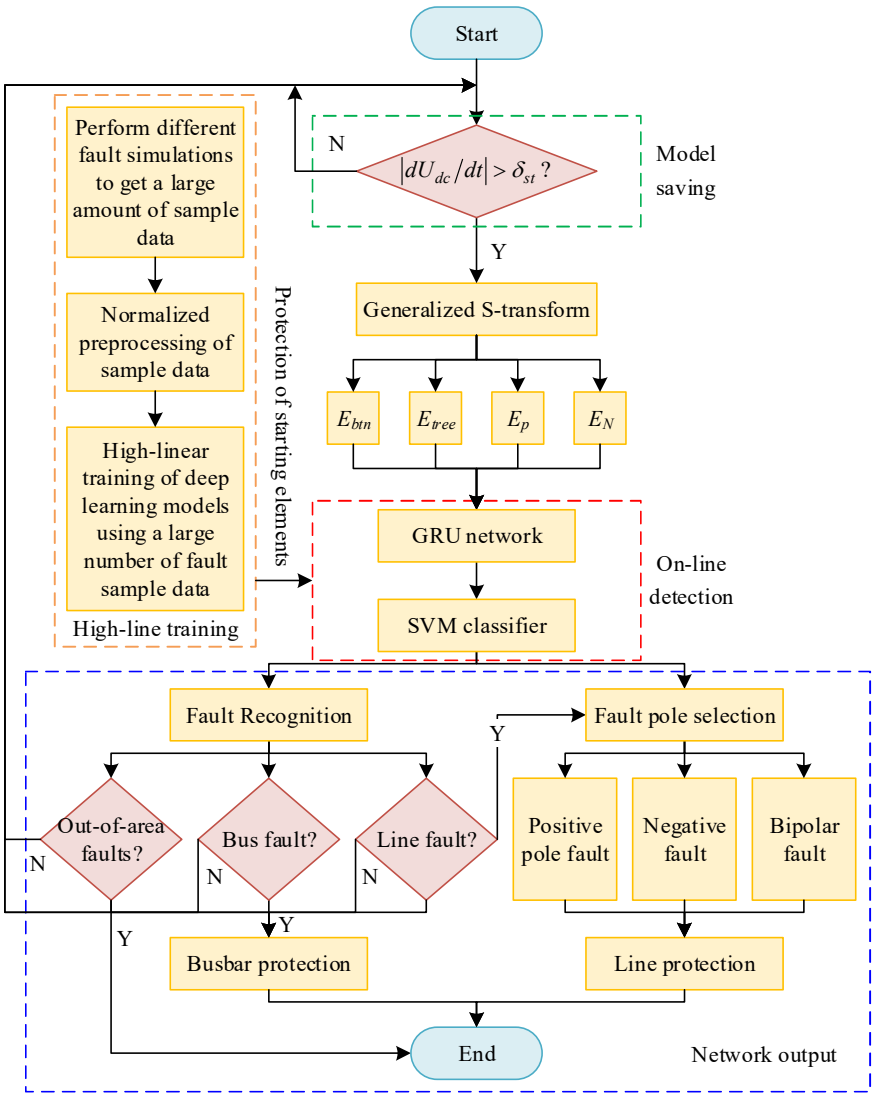

Figure 4: Protection scheme based on gated circulation unit network

In a science and technology enterprise park, there are single buildings such as production office building, expert apartment building, staff canteen, etc. In front of the staff canteen, there is an electric vehicle charging station, and solar photovoltaic power generation equipment is set up on the roof of the staff canteen and the roof of the expert apartment building, and there is an enterprise data center in the production office building. The production office building has 30 floors above ground and two floors below ground, with a building height of 120 meters. The first floor below ground is a garage and equipment rooms, and the floors above ground are offices, meeting rooms, laboratories and other rooms. The expert apartment is a multi-storey residential building with 9 floors above ground and 1 floor below ground. There are three units in the expert apartment, with two households on each floor of each unit. The staff canteen is three floors above ground with a building height of 16.1 meters.

III. B. System Failure Identification

III. B. 1) Busbar fault identification

The above simulation mainly verifies that the protection scheme designed in this paper can reliably recognize the faults in the zone and carry out fault pole selection, in order to verify the bus fault recognition capability based on the CRU model. A bus Bus1 ground fault is set up in a science and technology enterprise park, and the bus fault identification simulation results are shown in Fig. 5. As can be seen from the figure, it is found that Eline is greater than Ebus, and EP is greater than EN, at this time, the output of CRU model is R[0,1,0,0,0,1,0], which indicates that the CRU model recognizes the building DC distribution system fault as a bus negative fault, and all the circuit breakers close to this bus on the lines connected to it trip to remove the fault.

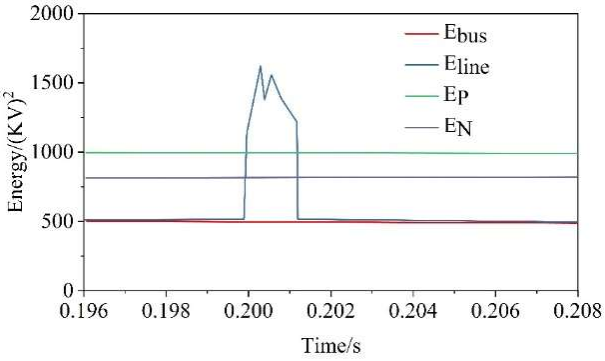

Figure 5: Bus fault identification simulation results

III. B. 2) Line fault identification

This subsection takes the distribution system line of a science and technology enterprise park as a test point, and Eline, Ebus, EP, and EN are put into the trained gated recurrent unit neural network to get the line fault detection results, and the simulation analysis of the distribution system line fault detection is shown in Fig. 6. Based on the data performance in the figure, it can be seen that when Eline is greater than Ebus, the corresponding EP is greater than EN, at this time, the fault detection model based on the gated recurrent unit neural network outputs R[1,0,0,1,0,0], and the corresponding fault detection result is the positive pole fault of the line, and the building distribution system sends out the tripping command, and the positive pole circuit breaker operates to remove the fault.

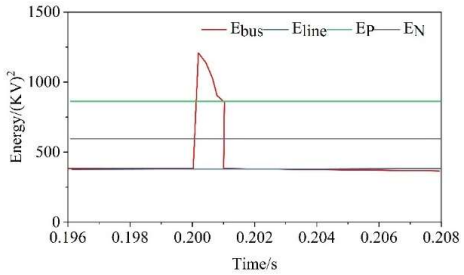

Figure 6: Distribution system line fault detection simulation analysis

III. B. 3) Out-of-area fault detection

Assuming that an out-of-area single-pole ground fault occurs in the construction project sample, the same method described above is adopted to detect the out-of-area fault for this sample, and the out-of-area fault detection results are shown in Fig. 7, with the horizontal axis being the time series and the vertical axis being the energy value. Through the data performance in Fig. 6, it can be seen that when Eline is greater than Ebus, the corresponding EP is equal to EN, and the output result of the fault detection model R is [0,0,1,0,0,0,0], and the corresponding type of fault is out-of-area fault, which verifies that the GRU network is capable of realizing the function of fault identification and fault pole selection of the building distribution system, and that the protection is correctly operated.

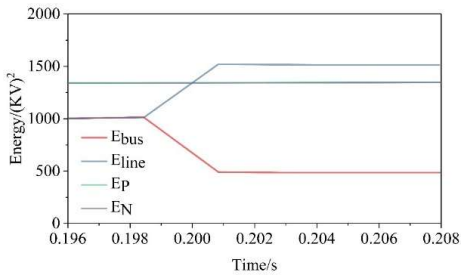

Figure 7: Out-of-area fault detection result

III. C. Identification of recognition effects of different models

In order to improve the reliability of the fault identification model of building distribution system based on GRU network, four groups of control models are set up, which are LSTM, CNN, RNN, and DNN. Combined with the value of evaluation indexes, the identification effect of different models is compared and analyzed.

III. C. 1) Evaluation indicators

At present, for the comparative analysis of recognition models, the commonly used evaluation indexes are accuracy, precision, and recall, and their corresponding formulas are shown below:

$$\text{Accuracy} = \frac{a_0 + a_1}{a_0 + a_1 + b_0 + b_1} \tag{15}$$

$$\text{Precision} = \frac{a_1}{a_1 + b_1} \tag{16}$$

$$\text{Recall rate} = \frac{a_1}{a_1 + b_0} \tag{17}$$

The correct numbers a_0 and a_1 indicate the number of correctly categorized types 0 and 1, respectively, while the incorrect number b_0 indicates the number of types that were originally classified as type 1 but were categorized as type 0, and b_1 indicates the number of types that were originally classified as type 0 but were categorized as type 1.

III. C. 2) Analysis of results

Using the evaluation indexes mentioned above, the identification effect of different models is compared and analyzed, and the comparison results of the identification effect of different models are shown in Fig. 8, where the horizontal axis corresponds to the six fault types (line fault R1, bus fault R2, out-of-area fault R3, positive fault R4, negative fault R5, and bipolar fault R6), and the vertical axis is the value of the evaluation indexes, in which (a) to (c) denote the accuracy rate and precision, respectively, Recall. The values of accuracy, precision, and recall of this paper's model are all between 0.85 and 0.95, and the performance of the six types of fault identification is more outstanding compared with the other four types of models, which further confirms that the GRU network in deep learning model has high priority in building distribution system fault identification, and provides guidance for intelligent fault diagnosis of building distribution system.

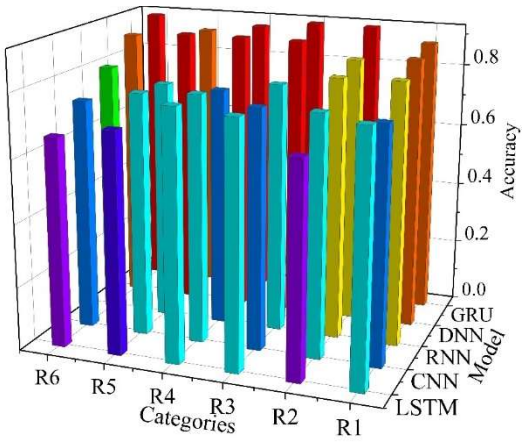

(a)Accuracy

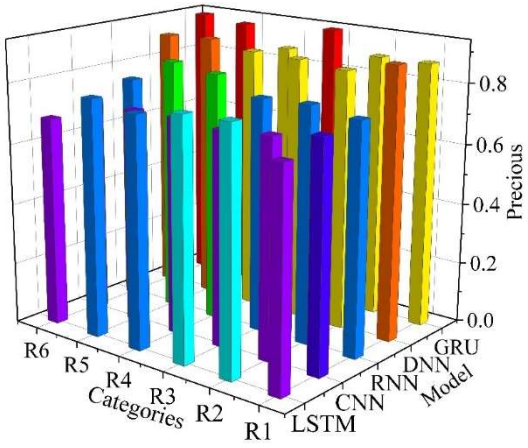

(b)Precision

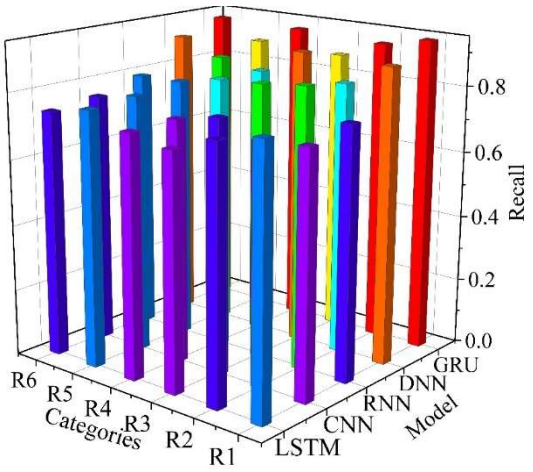

(c)Recall

Figure 8: Different model recognition results

III. D. Protection Program Validation Analysis

According to the above protection initiation criterion, it can be seen that the threshold value for initiating the GRU-based protection scheme for building DC distribution system is 0.35 ms. In this section, the out-of-area fault is mainly used as an example to verify the practical usefulness of the protection scheme in this paper, and the main content contains the simulation analysis of out-of-area fault protection, and the analysis of the impact of transition resistance.

III. D. 1) Out-of-area faults

Assuming that a single-pole grounding fault occurs on the out-of-area line in the science and technology park to verify the selectivity of the protection scheme, the simulation results of the out-of-area fault protection scheme are shown in Fig. 9, and (a) to (d) are the rate of change of the voltage at the right end, the rate of change of the voltage at the left end, and the ratio of the current and voltage, respectively. After the fault occurs, the zero mode voltage of the line increases, and in Fig. 9 (a) and (b), the rate of change of the zero mode voltage measured at the protection installation at the left and right ends of the faulty line tends to grow first and then decline, and the fault occurs at 0.35ms, and the rate of change of the zero mode voltage measured at the bus exceeds the protection startup threshold. In Fig. 9(c), after the fault protection scheme is activated, the line zero-mode differential current is calculated by the GRU model based on the measured zero-mode voltage and the in-zone and out-of-zone models, and the data time window is 1 ms, so that the GRU model outputs the first dU_{dc}/dt ratios after the fault occurs for 0.35 ms. The measured values of the line zero-mode differential current and the calculated values obtained based on the out-of-zone model have a high degree of similarity, while the measured values and the calculated values obtained based on the in-zone model have a low degree of similarity. From Fig. 9(d), it can be seen that the input is much larger than the output and the ratio of the two is much larger than 1. Therefore, the protection of the line reliably determines that the fault occurs outside the zone.

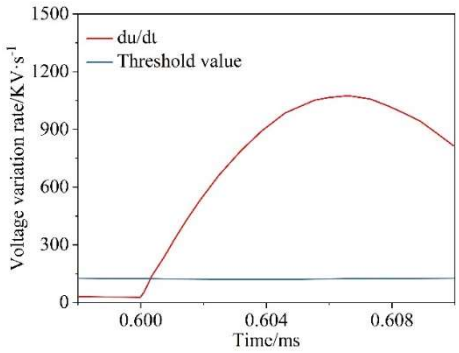

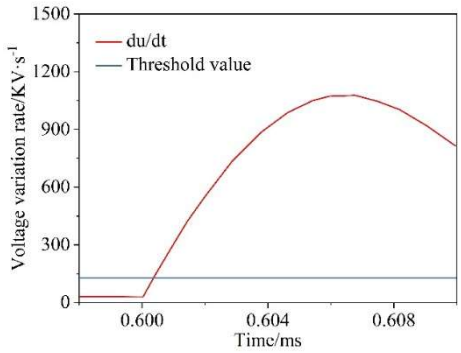

(a)Right (b)Left

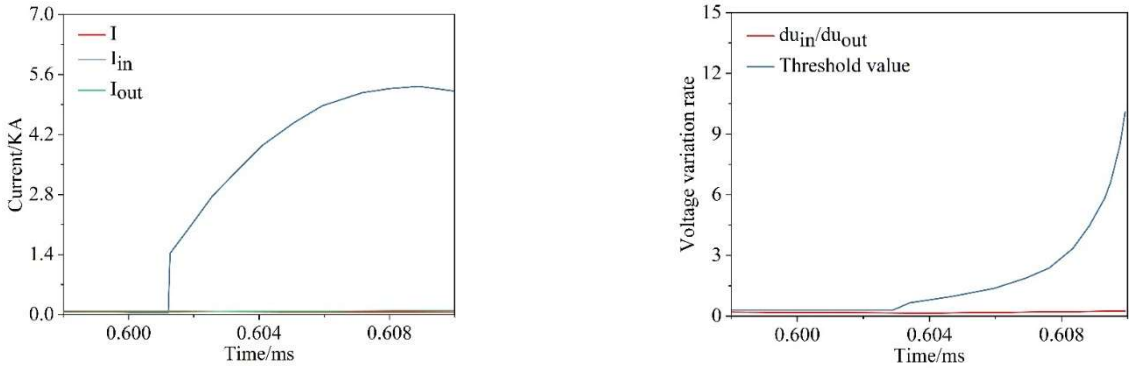

(c)Electric current (d)Voltage ratio

Figure 9: Simulation results of out-of-area fault protection scheme

III. D. 2) Effect of transition resistance

In order to verify the action of the protection under different fault points and different transition resistances, the following fault scenarios are set up in the simulation platform (bus, line, and out-of-area), and the simulation results of the effect of transition resistance are shown in Table 1. In the table, the voltage change rate ratio is the maximum value within 0.35ms after the protection start, in the three fault scenarios, as the fault transition resistance increases, even if there is a transition resistance of 100 Ω, the voltage change rate ratio is much less than 1, indicating that in the face of a stronger resistance to transition resistance, this paper can also play a good role in the protection of the building DC distribution system protection scheme.

Table 1: Effect of transition resistance on simulation results

Fault location	Transition resistance /Ω	Ratio of voltage change rate
Bus bar	0	0.00419
	50	1.092×10^{-4}
	100	1.784×10^{-4}
Line	0	0.00407
	50	1.151×10^{-4}
	100	1.377×10^{-4}
Out-of-area	0	0.00408
	50	1.392×10^{-4}
	100	1.279×10^{-4}

IV. Conclusion

In this paper, we design the DC power distribution system of a building, propose the fault variables of this system using the generalized S-transform, construct a gated cyclic unit network oriented to safety protection and fault identification, and validate and analyze the model by combining with the actual situation of a sample of the building project.

(1) The input values satisfy Eline>Ebus, EP>EN at the same time, and the CRU model fault identification result R[0,1,0,0,0,1,0], which indicates that at this time, the building DC distribution system exhibits a negative bus fault, and the model gives a circuit breaker tripping protection scheme.

(2) The three evaluation index values of this paper's model for six types of fault identification are maintained in the range of 0.85~0.95, which is particularly effective in fault identification relative to the other four types of models.

(3) Under the action of 0 Ω, 50 Ω and 100 Ω transition resistors, the ratio of the voltage change rate between input and output does not exceed 1, indicating that the protection scheme based on the CRU model still has good performance in the face of this type of situation.

Funding

This work is supported by the 2021 Guangxi Research Capacity Enhancement Program for Young and Middle-aged Teachers, under the project "Research on the Detection and Management of Power Quality in Civil Buildings" (Project No. 2021KY1077).

References

[1] Mackay, L., Blij, N. H. V. D., Ramirez-Elizondo, L., & Bauer, P. (2017). Toward the universal DC distribution system. Electric Power Components and Systems, 45(10), 1032-1042.

[2] Prabhala, V. A., Baddipadiga, B. P., Fajri, P., & Ferdowsi, M. (2018). An overview of direct current distribution system architectures & benefits. Energies, 11(9), 2463.

[3] Nasirian, V., Davoudi, A., Lewis, F. L., & Guerrero, J. M. (2014). Distributed adaptive droop control for DC distribution systems. IEEE Transactions on Energy Conversion, 29(4), 944-956.

[4] Feng, X., Qi, L., & Pan, J. (2017). A novel fault location method and algorithm for DC distribution protection. IEEE Transactions on Industry Applications, 53(3), 1834-1840.

[5] Kersting, W. H. (2018). Distribution system modeling and analysis. In Electric power generation, transmission, and distribution (pp. 26-1). CRC press.

[6] Lee, J. Y., Kim, H. S., & Jung, J. H. (2019). Enhanced dual-active-bridge DC–DC converter for balancing bipolar voltage level of DC distribution system. IEEE Transactions on Industrial Electronics, 67(12), 10399-10409.

[7] Mishra, R., Vaghasiya, K. M., & Agarwal, V. (2019, September). Improved modular multilevel converter with output voltage boosting capability for medium voltage DC distribution system. In 2019 IEEE Industry Applications Society Annual Meeting (pp. 1-6). IEEE.

[8] Jing, G., Zhang, A., & Zhang, H. (2018, November). Review on DC distribution network protection technology with distributed power supply. In 2018 Chinese Automation Congress (CAC) (pp. 3583-3586). IEEE.

[9] Farhadi, M., & Mohammed, O. A. (2017). Protection of multi-terminal and distributed DC systems: Design challenges and techniques. Electric Power Systems Research, 143, 715-727.

[10] Chandra, A., Singh, G. K., & Pant, V. (2020). Protection techniques for DC microgrid-A review. Electric Power Systems Research, 187, 106439.

[11] Sarangi, S., Sahu, B. K., & Rout, P. K. (2021). A comprehensive review of distribution generation integrated DC microgrid protection: issues, strategies, and future direction. International journal of energy research, 45(4), 5006-5031.

[12] Blaabjerg, F., Yang, Y., Yang, D., & Wang, X. (2017). Distributed power-generation systems and protection. Proceedings of the IEEE, 105(7), 1311-1331.

[13] Feng, X., Xiong, Q., Wardell, D., Gattozzi, A. L., Strank, S. M., & Hebner, R. E. (2019). Extra-fast DC distribution system protection for future energy systems. IEEE Transactions on industry applications, 55(4), 3421-3430.

[14] Wang, M., Abedrabbo, M., Leterme, W., Van Hertem, D., Spallarossa, C., Oukaili, S., ... & Kuroda, K. (2017, October). A review on ac and dc protection equipment and technologies: Towards multivendor solution. In CIGRE Winnipeg 2017 Colloquium (pp. 1-11). Cigré.

[15] Jia, K., Zhao, Q., Feng, T., & Bi, T. (2019). Distance protection scheme for DC distribution systems based on the high-frequency characteristics of faults. IEEE Transactions on Power Delivery, 35(1), 234-243.

[16] Xiong, Q., Feng, X., Gattozzi, A. L., Liu, X., Zheng, L., Zhu, L., ... & Hebner, R. E. (2019). Series arc fault detection and localization in DC distribution system. IEEE Transactions on Instrumentation and Measurement, 69(1), 122-134.

[17] Hallemans, L., Van den Broeck, G., Ravyts, S., Alam, M. M., Dalla Vecchia, M., Van Tichelen, P., & Driesen, J. (2019, May). Fault identification and interruption methods in low voltage dc grids—A review. In 2019 IEEE Third International Conference on DC Microgrids (ICDCM) (pp. 1-8). IEEE.

[18] Oh, Y. S., Kim, C. H., Gwon, G. H., Noh, C. H., Bukhari, S. B. A., Haider, R., & Gush, T. (2019). Fault detection scheme based on mathematical morphology in last mile radial low voltage DC distribution networks. International Journal of Electrical Power & Energy Systems, 106, 520-527.

[19] Mohanty, R., & Pradhan, A. K. (2018). Faulted section identification for DC distribution systems using smart meter data. IET Generation, Transmission & Distribution, 12(4), 1030-1037.

[20] Dhar, S., Patnaik, R. K., & Dash, P. K. (2017). Fault detection and location of photovoltaic based DC microgrid using differential protection strategy. IEEE Transactions on Smart Grid, 9(5), 4303-4312.

[21] Bhargav, R., Bhalja, B. R., & Gupta, C. P. (2019). Novel fault detection and localization algorithm for low-voltage DC microgrid. IEEE Transactions on Industrial Informatics, 16(7), 4498-4511.

[22] Xu, Y., Liu, J., Jin, W., Fu, Y., & Yang, H. (2018). Fault location method for dc distribution systems based on parameter identification. Energies, 11(8), 1983.

[23] Geddada, N., Yeap, Y. M., & Ukil, A. (2017). Experimental validation of fault identification in VSC-based DC grid system. IEEE Transactions on Industrial Electronics, 65(6), 4799-4809.

[24] Nana Jia,Tong Jia & Zhiao Zhang. (2025). A residual GRU method with deep cross fusion for Alzheimer's disease progression prediction using missing variable-length time series data. Biomedical Signal Processing and Control107253-107253.

[25] Mehmet Bilgili,Engin Pinar & Tahir Durhasan. (2024). Global monthly sea surface temperature forecasting using the SARIMA, LSTM, and GRU models. Earth Science Informatics(1),10-10.

[26] Wang Jiechen,Gao Zhimei & Ma Yan. (2022). Prediction Model of Hydropower Generation and Its Economic Benefits Based on EEMD-ADAM-GRU Fusion Model. Water(23),3896-3896.

[27] Md. Mahfuz Ahmed,Md. Maruf Hossain,Md. Rakibul Islam,Md. Shahin Ali,Abdullah Al Noman Nafi,Md. Faisal Ahmed... & Md. Khairul Islam. (2024). Brain tumor detection and classification in MRI using hybrid ViT and GRU model with explainable AI in Southern Bangladesh. Scientific Reports(1),22797-22797.